Three-dimensional slope stability under tri-directional pseudo-static seismic loading

Sharma, V[1][0000-0003-3412-2762] and Raj, D.[1][0000-0002-5296-8588]

[1] Department of Civil Engineering, MNIT Jaipur, Jaipur 302017, Rajasthan, India
dhiraj.ce@mnit.ac.in

Abstract. In reality, the constitutive materials of natural slope are quite heterogeneous. The materials are assumed as homogeneous, isotropic and uniformly distributed in horizontal direction for a two-dimensional analysis of slope, which is an oversimplification of an actual case. However, a three-dimensional analysis for slope is preferred in such case where slopes have complex geometry including sharp ridges, corners, cut and fill slopes, unplanned excavations, etc, constitutive materials are heterogeneous (varying along depth and along out of plane direction) and slopes subjected to seepage and seismic loadings.

In this article, a numerical study has been conducted to obtain the FOS of four generic three-dimensional slopes. Finite element analyses have been performed for three dimensional slopes using the proprietary software ABAQUS following the strength reduction method. The seismic loads have been applied in simplified pseudo-static form in three mutually perpendicular directions to estimate the FOS of 3-D slopes having complex geometry. A parametric study has been carried out on four slopes having same cross section, soil property and boundary conditions with varying geometry to understand the variation in FOS and failure surface with changing complex geometry. It was apparent that on increasing the seismic coefficients, FOS kept on reducing.

Keywords: 3D slope stability; Strength reduction method; Tri-directional seismic load.

1   Introduction

The Himalayan range spans through eleven states and two union territories in the Indian mainland. People from relatively flat-landscape cities have long been attracted towards these hilly locations for rest, recuperation and recreational activities. To fulfill the demands of floating population, the hilly regions have faced a lot of construction activities, in recent time. These structures include residential apartments, villas, commercial hotels, and shopping malls as well as public utilities such as towers for telecommunication and power distribution and aerial ropeways. Majority of these hilly areas are

heavily populated and the buildings are placed next to each other. In addition, these hilly areas are also located in seismically active zones, e.g., Shimla (Himachal Pradesh) and Nainital (Uttarakhand) both are located in seismic zone IV. In the past, several deadly landslides occurred in the hilly region of India during the Assam Earthquake, 1897 (M_w = 8.1), Assam Earthquake, 1950 (M_w = 8.6), Uttarkashi Earthquake, 1991 (M_w = 6.6), Chamoli Earthquake, 1999 (M_w = 6.4) and Kashmir Earthquake, 2005 (M_w = 7.6) and Sikkim Earthquake, 2011 (M_w = 6.9) [1]. There are two main factors which contribute to slope instability in mountainous terrains: (a) an increase in applied stress and (b) a decrease in the strength of the constitutive materials of the slope [2]. The hilly regions of India, falling in the Himalayan belt, have varying topography ranging from very high mountains, height sometimes exceeding twenty thousand feet, to as low as areas lying near mean sea level, including plateau like regions [3]. In these regions, the occurrence of landslides due to seismic action may be an output of interaction of several factors such as magnitude of the prevailing seismic activity, depth of epicenter, place of fault plane. The tendency of the slope to fail is also dependent on the angle of inclination of slope and height from top to base of slope [3].

Previously, a number of researchers [4-8] have utilized limit equilibrium approach to analyze the stability of two-dimensional slopes. Most of the time, in 2-D slope stability analysis the slope is assumed to be composed of homogeneous and isotropic materials which are further assumed to be horizontally distributed in an out-of-plane direction, and slopes are subjected to planer loading (such as seismic load, imposed load from the structure, pore water pressure, etc.), which rarely exist in real field conditions. When the slope geometry is complex (includes narrow failure surfaces, ridges or corners, slopes cut by excavations, etc.) and consists of heterogeneous and anisotropic material with significant changes in out of plane direction, the existing 2-D methods are ineffective and 3-D analysis is required to deal with such conditions. Most of the past studies [9-15] have found that for a same slope, the factor of safety (FoS) obtained for a slope in 2-D analysis is lesser than the FoS estimated from 3-D analysis. In order to simplify the nature of the 3-D seismic slope stability analysis, sometimes previous researchers [16-18] have ignored the effect of vertical acceleration stating that the peak values of the horizontal and vertical accelerations rarely occur at the same time, and the vertical acceleration is typically out of phase with the horizontal component and has a distinct frequency content.

In this paper, a numerical investigation has been carried out to access the stability of the 3-D slope subjected to generalized seismic load (applied in all three direction). utilizing the simplified pseudo-static method. To obtain the failure surface and FoS, the strength reduction technique has been implemented in finite element framework with the proprietary software ABAQUS [19]. Four typical slopes with varying 3-D geometries, but similar 2-D cross-sections, soil parameters, and boundary conditions have been used in a parametric analysis. The results are presented in the form of variation in FoS with the horizontal seismic coefficient (α_h) applied in both lateral directions and vertical seismic coefficient (α_v) applied in the direction perpendicular to both lateral directions.

2   Numerical Study

In the current study, four homogeneous slopes with the same cross-sectional properties, i.e. slope angle, $\beta = 26.57°$ (2H:1V), and slope height, $H = 12$ m, have been considered. The 3-D geometry of the considered four slopes: (a) convex 90˚ slope; (b) concave 90˚ slope; (c) convex turning arc 90˚ slope and (d) concave turning arc 90˚ slope, is shown in Fig. 2. The material properties of soil, used in this investigation, is shown in Table 1.

Table 1. Soil Properties [20]

S.No.	Property	Value
1	Cohesion, c	29000 Pa
2	Friction angle (ϕ)	20˚
3	Unit weight of soil (γ)	18.44 kN/m³
4	Youngs Modulus (E)	10 MPa
5	Poisson's Ratio (v)	0.25

(a)

(c)

(b)

(d)

s
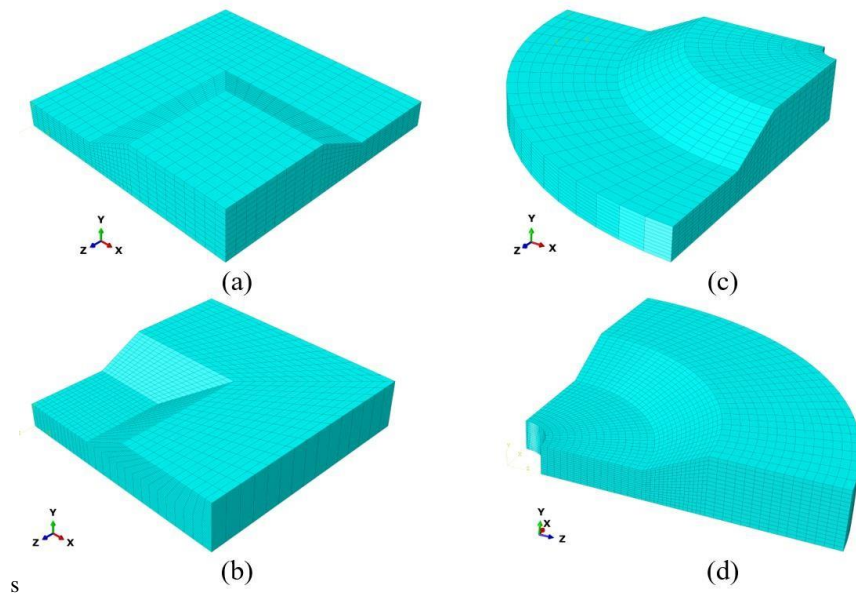
Fig. 1. 3D geometry of: (a) convex 90˚ slope; (b) concave 90˚ slope; (c) convex turning arc 90˚ slope; (d) concave turning arc 90˚ slope.

TH-6-74

This study has been conducted to understand the change in FoS and the failure surface of the considered slopes subjected to the different seismic loading combinations (taken as per the recommendation of IS 1893 (Part 1): 2016 [21] along with constant action of gravity.

3　FE Modeling and Analysis

To determine the FoS of the slopes under consideration under tri-directional seismic loading, 3-D finite element analysis (FEA) based on the strength reduction method (SRM) has been carried out using ABAQUS [19]. In strength reduction method (SRM), the initial material strength parameters were decreased by a strength reduction factor at each successive step [22-24] and the factor corresponding to instable slope has been refereed as FoS. By following the method of Xu et al. [25], the current SRM has been altered and implemented in ABAQUS through addition of a field variable, which represents an incremental step time and a controlling parameter which decrease the strength parameters (c and ϕ) of the soil in successive steps.

A non-associated flow rule along with Mohr-Coulomb failure criterion was used in the analyses in order to describe the elasto-plastic nature of the soil model. The soil mass, modelled as three-dimensional finite element, has been discretized with eight noded brick elements with reduced integration (C3D8R), available in ABAQUS's elements library (as shown in Fig. 1). To ensure the insignificant effect of boundary conditions on the FoS of slope, the lateral extent of the FE model has been taken based on sensitivity study and recommendations from the previous studies. The movement of sides and bottom face of the FE model have been restricted in all direction, whereas the movement of the front and back faces of slope have been restricted in normal direction only [20]. With these boundary conditions, the results obtained from the above mentioned method agrees well with the work of Zhang et al [20].

All the considered slopes have been analyzed under gravity loading along with different linear combinations of seismic loading as per IS 1893 (Part 1): 2016. The combinations of seismic loading applied on the slope are either varying uni-directional (α_{hx} or α_{hz} or $+\alpha_{vy}$ or $-\alpha_{vy}$) loading or varying tri-directional ($\alpha_{hx} + \alpha_{vy} + \alpha_{hz}$; $\alpha_{hx} + 0.3 \times \alpha_{vy} + 0.3 \times \alpha_{hz}$; $0.3 \times \alpha_{hx} + \alpha_{vy} + 0.3 \times \alpha_{hz}$ and $0.3 \times \alpha_{hx} + 0.3 \times \alpha_{vy} + \alpha_{hz}$) loading, in multiple steps which yielded a total one hundred and five number of analyses for each 3D slope. All of these slopes have been analyzed upto the critical acceleration (α_c) as defined by Newmark [26]:

$$\alpha_c = (\text{FoS}_S - 1) \times g \times \sin \beta \qquad (1)$$

where, FoS_S = Static factor of safety, g = acceleration due to gravity, β = slope angle.

4 Results and Discussions

The primary objective of this research is to explore about the failure surface and variation in FoS of four distinct complex 3-D slopes (convex 90˚ slope, concave 90˚ slope, convex turning arc 90˚ slope, and concave turning arc 90˚ slope) under the combined effect of gravity and tri-directional seismic loading. The following section discuss the results of the current investigation.

Figure 2(a-d) and 2(e-h) shows the failure surface represented by strain rate (ER) profile for convex 90˚ slope and concave 90˚ slope under gravity load only and additionally subjected to different linear seismic load combinations, $\alpha_{vy} = 0.3$g, $\alpha_{hx} = \alpha_{hz} = 0.09$g; $\alpha_{hx} = 0.3$g, $\alpha_{vy} = \alpha_{hz} = 0.09$g; and $\alpha_{vy} = \alpha_{hx} = \alpha_{hz} = 0.3$g, respectively. Similarly, Figures 3(a-d) and 3(e-h) show the failure surface for convex turning arc 90˚ slope and concave turning arc 90˚ slope, under gravity load along with different linear seismic load combinations, $\alpha_{vy} = 0.3$g, $\alpha_{hx} = \alpha_{hz} = 0.09$g; $\alpha_{hx} = 0.3$g, $\alpha_{vy} = \alpha_{hz} = 0.09$g; and $\alpha_{vy} = \alpha_{hx} = \alpha_{hz} = 0.3$g, respectively. It can be observed from the figure that in all of the considered cases, the value of FoS reduces significantly for the slope subjected to increasing seismic load combinations as compared to the slope under gravity load only. It can also be noted that the in all the cases failure surfaces are symmetric and change with increasing seismic load combinations, except in figures 2(c & g) and 3(c & g) where the failure surfaces are asymmetric.

Fig. 4(a-d) shows the variation in FoS for convex 90˚ slopes, concave 90˚ slopes, convex 90˚ turning arc slope and concave 90˚ turning arc slope, respectively, with increasing uni-directional (α_{hx} or α_{hz} or $+\alpha_{vy}$ or $-\alpha_{vy}$) loading or tri-directional seismic load combinations ($\alpha_{hx} + 0.3 \times \alpha_{vy} + 0.3 \times \alpha_{hz}$; $\alpha_{hx} + \alpha_{vy} + \alpha_{hz}$; $0.3 \times \alpha_{hx} + \alpha_{vy} + 0.3 \times \alpha_{hz}$; $0.3 \times \alpha_{hx} + 0.3 \times \alpha_{vy} + \alpha_{hz}$) applied in multiple steps.

It can be noted that, FoS has been reduced significantly under the combination of increasing horizontal (α_{hx} and α_{hz}) and vertical (α_{vy}) seismic coefficients, in all the cases. However, a marginal decreasing effect has been observed in case of slope subjected to vertical (α_{vy}) seismic coefficient applied in the direction of gravity. Further, when the slope was subjected to increasing vertical (α_{vy}) seismic coefficient applied in the opposite direction of gravity, FoS has also been found increasing. This observation is consistent with the past studies [16-18], where the average seismic response of the system was observed to be rather insensitive to positive and negative contributions from the vertical acceleration and recommended to ignore the contribution of vertical acceleration.
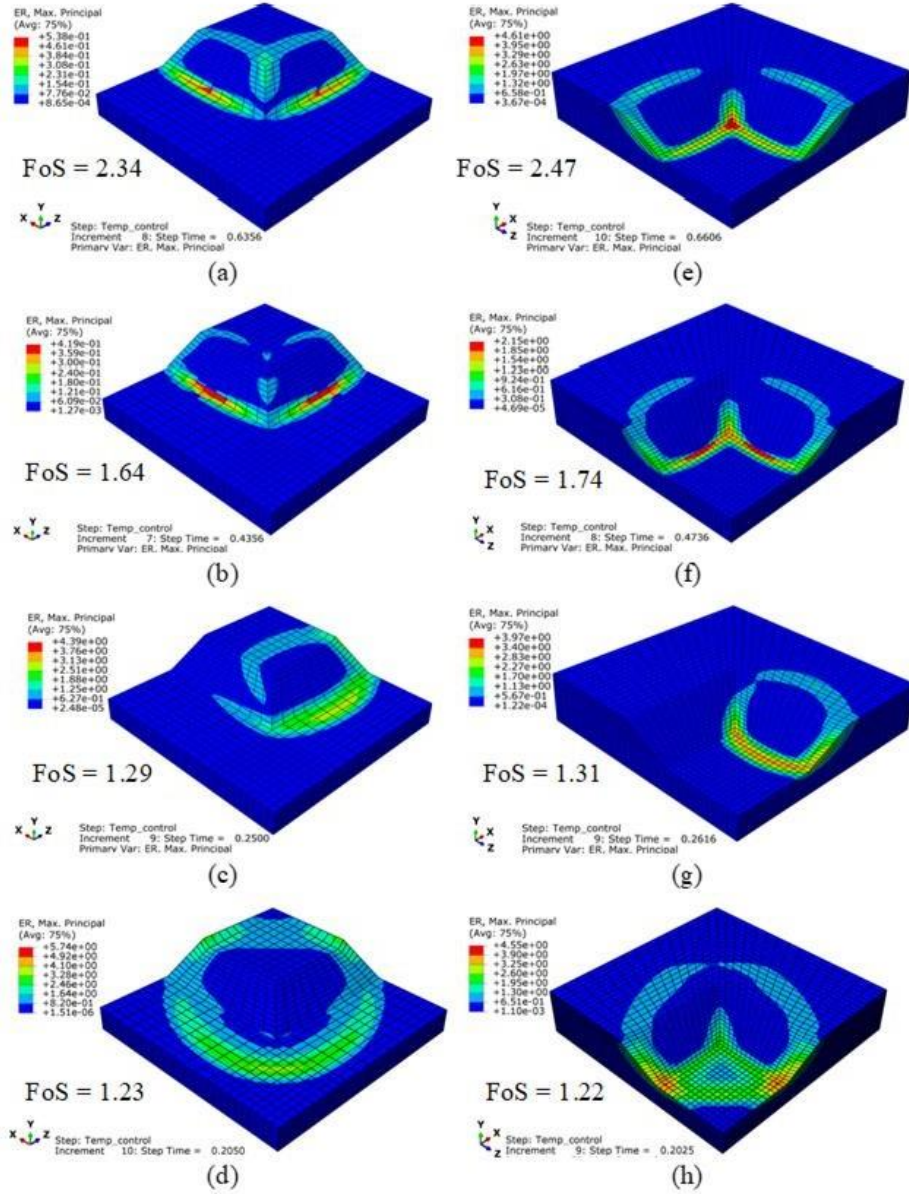
Fig. 2. Strain rate (ER) profile representing the failure surface for: (a) convex 90˚ slope under gravity load only, (b) convex 90˚ slope subjected to $\alpha_{vy} = 0.3g$, $\alpha_{hx} = \alpha_{hz} = 0.09g$, (c) convex 90˚ slope subjected to $\alpha_{hx} = 0.3g$, $\alpha_{vy} = \alpha_{hz} = 0.09g$, (d) convex 90˚ slope subjected to $\alpha_{vy} = \alpha_{hx} = \alpha_{hz} = 0.3g$, (e) concave 90˚ slope under gravity load only, (f) concave 90˚ slope subjected to $\alpha_{vy} = 0.3g$, $\alpha_{hx} = \alpha_{hz} = 0.09g$, (g) concave 90˚ slope subjected to $\alpha_{hx} = 0.3g$, $\alpha_{vy} = \alpha_{hz} = 0.09g$, (h) concave 90˚ slope subjected to $\alpha_{vy} = \alpha_{hx} = \alpha_{hz} = 0.3g$.

TH-6-74
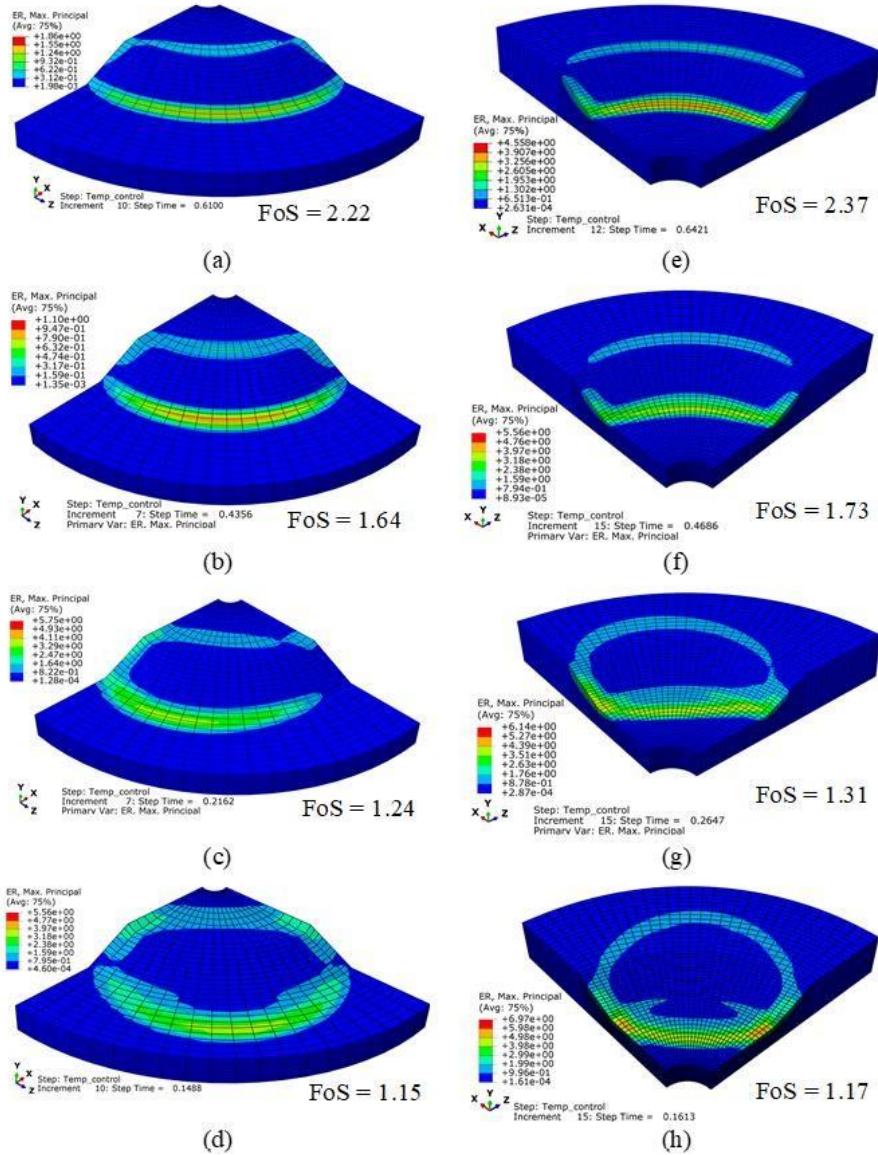
Fig. 3. Strain rate (ER) profile representing the failure surface for: (a) convex turning arc 90° slope under gravity load only, (b) convex turning arc 90° slope subjected to $\alpha_{vy} = 0.3g$, $\alpha_{hx} = \alpha_{hz} = 0.09g$, (c) convex turning arc 90° slope subjected to $\alpha_{hx} = 0.3g$, $\alpha_{vy} = \alpha_{hz} = 0.09g$, (d) convex turning arc 90° slope subjected to $\alpha_{vy} = \alpha_{hx} = \alpha_{hz} = 0.3g$, (e) concave turning arc 90° slope under gravity load only, (f) concave turning arc 90° slope subjected to $\alpha_{vy} = 0.3g$, $\alpha_{hx} = \alpha_{hz} = 0.09g$, (g) concave turning arc 90° slope subjected to $\alpha_{hx} = 0.3g$, $\alpha_{vy} = \alpha_{hz} = 0.09g$, (h) concave turning arc 90° slope subjected to $\alpha_{vy} = \alpha_{hx} = \alpha_{hz} = 0.3g$

7

TH-6-74
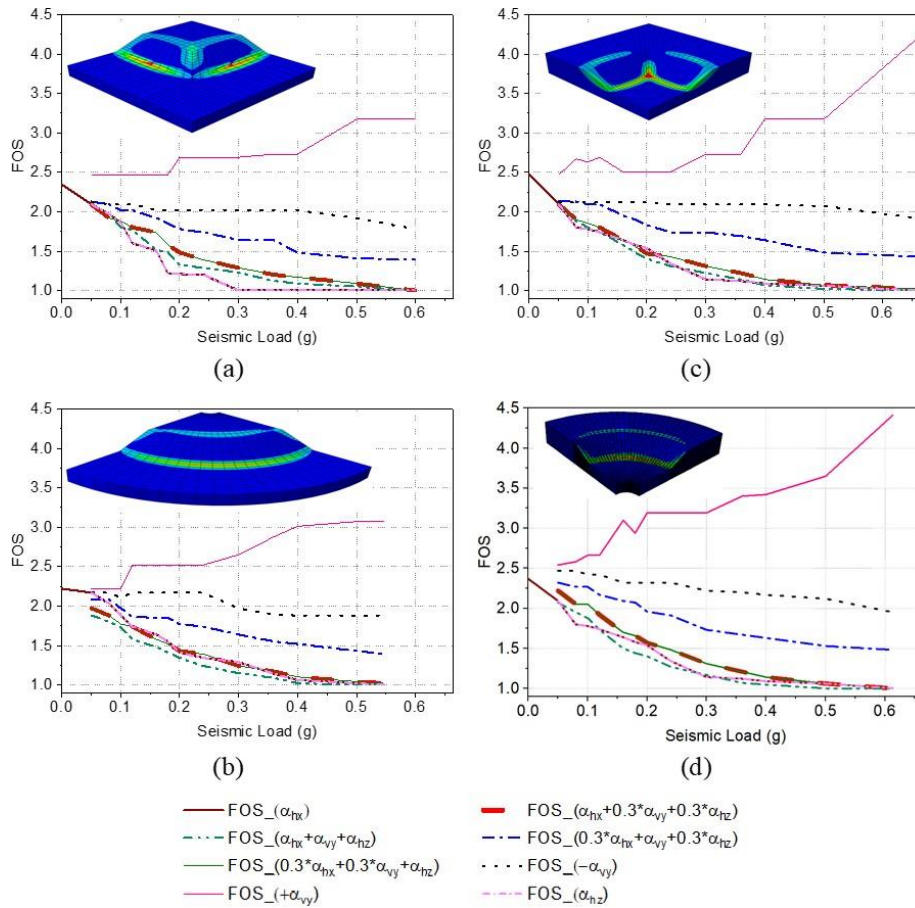
Fig. 4. Variation in FoS with horizontal (α_{hx}, α_{hz}) and vertical seismic coefficients (α_{vy}) for: (a) convex 90˚ slope; (b) convex turning arc 90˚ slope; (c) concave 90˚ slope; and (d) concave turning arc 90˚ slope; (e) legend.

5   Conclusions

In this article, a parametric analysis has been conducted to comprehend the behaviour of 3-D slopes with distinct complex geometries, having similar 2-D cross-sections, soil parameters, and boundary conditions, when subjected to tri-directional seismic loads. A modified strength reduction technique is implemented in the ABAQUS finite element software in order to obtain the FoS of the slopes. It was observed that the shape of the failure surface varies with the applied horizontal and vertical seismic coefficients. As

expected, the FoS was found to be decreasing with increasing horizontal and vertical seismic coefficients, in either direction or in combination, in most of the cases. Except in the case, when the slope was subjected to increasing vertical seismic coefficient in the positive (upward direction) only, the FoS was also observed to be increasing. The present analysis has been performed by assuming the slope consists of homogenous material, having generic 3-D geometry and subjected to simplified pseudostatic seismic force; hence the result is restricted to the investigated case only. For more realistic understanding, a comprehensive study is required including dynamic analysis of slope with time-varying shear strength and natural slope geometry.

6   Acknowledgments

References

1. Singh H., Som S.K.: Earthquake triggered landslide–Indian scenario. Journal of the Geological Society of India 87(1), 105-111 (2016).
2. Duncan J.: State of the art: Limit equilibrium and finite-element analysis of slopes. Journal of Geotechnical Engineering 122(7), 577-596 (1996).
3. Parkash S.: Earthquake Related Landslides in the Indian Himalaya: Experiences from the Past and Implications for the Future. In: Catani F. M. C., Trigila A., Iadanza C. (ed) The Second World Landslide Forum 2011, vol 5, pp. 327-334. ISPRA - Italian National Institute for Environmental Protection and Research, Rome, (2011).
4. Bishop A.W.: The use of the slip circle in the stability analysis of slopes. Géotechnique 5(1), 7-17 (1955).
5. Morgenstern N.R., Price V.E.: The analysis of the stability of general slip surfaces. Géotechnique 15(1), 79-93 (1965).
6. Spencer E.: A method of analysis of the stability of embankments assuming parallel interslice forces. Géotechnique 17(1), 11-26 (1967).
7. Janbu N.: Slope stability computations. In: Hirschfeld R. C., Poulos S. J. (eds) Embankment-Dam Engineering - Casagrande Volume. pp. 47-86. John Wiley and Sons, Inc., New York, (1973).
8. Sarma S.K.: Stability analysis of embankments and slopes. Géotechnique 23(3), 423-433 (1973).
9. Baligh M.M., Azzouz A.S.: End Effects on Stability of Cohesive Slopes. Journal of the Geotechnical Engineering Division 101(11), 1105-1117 (1975).
10. Giger M.W., Krizek R.J.: Stability analysis of vertical cut with variable corner angle. Soils and Foundations 15(2), 63-71 (1975).

Sharma, V. and Raj, D.

11. Leshchinsky D., Baker R., Silver M.L.: Three dimensional analysis of slope stability. International Journal for Numerical and Analytical Methods in Geomechanics 9(3), 199-223 (1985).

12. Cavounidis S.: On the ratio of factors of safety in slope stability analyses. Géotechnique 37(2), 207-210 (1987).

13. Hungr O.: An extension of Bishop's simplified method of slope stability analysis to three dimensions. Géotechnique 37(1), 113-117 (1987).

14. Chen Z., Wang X., Haberfield C., Yin J.H., Wang Y.: A three-dimensional slope stability analysis method using the upper bound theorem: Part I: theory and methods. International Journal of Rock Mechanics and Mining Sciences 38(3), 369-378 (2001).

15. Chugh A.K.: On the boundary conditions in slope stability analysis. International Journal for Numerical and Analytical Methods in Geomechanics 27(11), 905-926 (2003).

16. Conti R.: Simplified formulas for the seismic bearing capacity of shallow strip foundations. Soil Dynamics and Earthquake Engineering 104(Supplement C), 64-74 (2018).

17. Huang C.C.: Seismic displacements of soil retaining walls situated on slope. Journal of Geotechnical and Geoenvironmental Engineering 131(9), 1108-1117 (2005).

18. Gazetas G., Psarropoulos P.N., Anastasopoulos I., Gerolymos N.: Seismic behaviour of flexible retaining systems subjected to short-duration moderately strong excitation. Soil Dynamics and Earthquake Engineering 24(7), 537-550 (2004).

19. ABAQUS. ABAQUS Documentation. Dassault Systèmes, Providence, RI, USA (2016).

20. Zhang Y.B., Chen G.Q., Zheng L., Li Y., Zhuang X.J.C.G.J.: Effects of geometries on three-dimensional slope stability. Canadian Geotechnical Journal 50(3), 233-249 (2013).

21. BIS. IS1893: Crieteria for Eathquake Resistance Design of Structures, Part 1 General Provisons and Buildings. Bureau of Indian Standard, New Delhi (2016).

22. Dawson E.M., Roth W.H., Drescher A.: Slope stability analysis by strength reduction. Géotechnique 49(6), 835-840 (1999).

23. Griffiths D.V., Lane P.A.: Slope stability analysis by finite elements. Géotechnique 49(3), 387-403 (1999).

24. Raj D., Singh Y., Kaynia A.M.: Behavior of slopes under multiple adjacent footings and buildings. International Journal of Geomechanics 18(7), 04018062 (2018).

25. Xu Q., Yin H., Cao X., Li Z.: A temperature-driven strength reduction method for slope stability analysis. Mechanics Research Communications 36(2), 224-231 (2009).

26. Newmark N.M.: Effects of Earthquakes on Dams and Embankments. Géotechnique 15(2), 139-160 (1965).